jove

A Lightweight Drive Implant for Chronic Tetrode Recordings in Juvenile Mice

Robert J. Pendry[1,2], **Lilyana D. Quigley**[1,2], **Lenora J. Volk**[1,3,4], **Brad E. Pfeiffer**[1,3]

[1] Department of Neuroscience, UT Southwestern Medical Center [2] Neuroscience Graduate Program, UT Southwestern Medical Center [3] O'Donnell Brain Institute, UT Southwestern Medical Center [4] Department of Psychiatry, UT Southwestern Medical Center

Corresponding Author

Brad E. Pfeiffer
Brad.Pfeiffer@UTSouthwestern.edu

Citation

Pendry, R.J., Quigley, L.D., Volk, L.J., Pfeiffer, B.E. A Lightweight Drive Implant for Chronic Tetrode Recordings in Juvenile Mice. *J. Vis. Exp.* (196), e65228, doi:10.3791/65228 (2023).

Date Published

June 2, 2023

DOI

10.3791/65228

URL

jove.com/video/65228

Abstract

In vivo electrophysiology provides unparalleled insight into the sub-second-level circuit dynamics of the intact brain and represents a method of particular importance for studying mouse models of human neuropsychiatric disorders. However, such methods often require large cranial implants, which cannot be used in mice at early developmental time points. As such, virtually no studies of *in vivo* physiology have been performed in freely behaving infant or juvenile mice, despite the fact that a better understanding of neurological development in this critical window would likely provide unique insights into age-dependent developmental disorders such as autism or schizophrenia. Here, a micro-drive design, surgical implantation procedure, and post-surgery recovery strategy are described that allow for chronic field and single-unit recordings from multiple brain regions simultaneously in mice as they age from postnatal day 20 (p20) to postnatal day 60 (p60) and beyond, a time window roughly corresponding to the human ages of 2 years old through to adulthood. The number of recording electrodes and final recording sites can be easily modified and expanded, thus allowing flexible experimental control of the *in vivo* monitoring of behavior- or disease-relevant brain regions across development.

Introduction

The brain undergoes large-scale changes during the critical developmental windows of childhood and adolescence[1,2,3]. Many neurologic and psychiatric diseases, including autism and schizophrenia, first manifest behaviorally and biologically during this period of juvenile and adolescent brain development[4,5,6]. While much is known regarding the cellular, synaptic, and genetic changes that occur across early development, comparatively little is known regarding how circuit- or network-level processes change throughout this time window. Importantly, circuit-level brain function, which ultimately underlies complex behaviors, memory, and cognition, is a non-predictable, emergent property of cellular and synaptic function[7,8,9,10]. Thus, to fully understand network-level brain function, it is necessary to directly study

neural activity at the level of an intact neural circuit. In addition, to identify how brain activity is altered throughout the progression of neuropsychiatric disorders, it is critical to examine network activity in a valid disease model during the specific temporal window when the behavioral phenotypes of the disease manifest and to track the observed changes as they persist into adulthood.

One of the most common and powerful scientific model organisms is the mouse, with large numbers of unique genetic strains that model neurodevelopmental disorders with age-dependent onset of the behavioral and/or mnemonic phenotypes[11,12,13,14,15,16,17,18,19,20,21]. While it is challenging to correlate precise developmental time points between the brains of humans and mice, morphological and behavioral comparisons indicate that p20-p21 mice represent the human ages of 2-3 years old, and p25-p35 mice represent the human ages of 11-14 years old, with mice likely reaching the developmental equivalent of a human 20 year old adult by p60[3,22]. Thus, to better understand how the juvenile brain develops and to identify how the neural networks of the brain become dysfunctional in diseases like autism or schizophrenia, it would be ideal to directly monitor brain activity *in vivo* in mice across the ages of 20 days to 60 days old.

However, a fundamental challenge in monitoring brain activity across early development in mice is the small size and relative weakness of juvenile mice. The chronic implantation of electrodes, which is necessary for longitudinal studies of brain development, typically requires large, bulky housing to protect the fine electrode wires and interface boards[23,24], and the implants must be firmly attached to the mouse skull, which is thinner and less rigid in young mice due to reduced ossification. Thus, virtually all studies of *in vivo* rodent physiology have been performed in adult subjects due to their relative size, strength, and skull thickness. To date, most studies exploring *in vivo* juvenile rodent brain physiology have been performed in wild-type juvenile rats, which necessarily limits the ability to experimentally monitor juvenile brain function in a freely behaving model of a human disorder[25,26,27,28,29,30].

This manuscript describes novel implant housing, a surgical implantation procedure, and a post-surgery recovery strategy to chronically study the long-term (up to 4 or more weeks) *in vivo* brain function of juvenile mice across a developmentally critical time window (p20 to p60 and beyond). The implantation procedure allows for the reliable, permanent affixation of the electrodes to the skulls of juvenile mice. Furthermore, the micro-drive design is lightweight, as this micro-drive weighs ~4-6 g when fully assembled, and due to the minimal counterbalancing required to offset the weight of the implant, it does not impact the behavioral performance of juvenile mice during typical behavioral paradigms.

Protocol

The present study was approved by the University of Texas Southwestern Medical Center Institutional Animal Care and Use Committee (protocol 2015-100867) and performed in compliance with both institutional and National Institute of Health guidelines. The C57/Bl6 male and female mice used in the present study were implanted at p20 (weight 8.3-11.1 g at the time of implantation).

1. Micro-drive design and construction

1. Digitally designing and printing the micro-drive (**Figure 1**)

1. Download the micro-drive model templates (https://github.com/Brad-E-Pfeiffer/JuvenileMouseMicroDrive).
2. Identify the stereotaxic locations of the target brain region(s) in an appropriate stereotaxic atlas.
3. Using three-dimensional computer-aided design (3D CAD) software, load the template micro-drive cannula (**Figure 1B**).
4. If necessary, modify the output cannula output locations on the micro-drive cannula model to target the desired brain region(s).
   NOTE: Each cannula hole extrusion should be at least 2 mm long to ensure that the tetrode will emerge from the cannula hole aiming straight at the target. The micro-drive cannula template is designed to bilaterally target the anterior cingulate cortex (one tetrode per hemisphere), hippocampal area CA1 (four tetrodes per hemisphere), and hippocampal area CA3 (two tetrodes per hemisphere), with one reference tetrode per hemisphere positioned in the white matter above hippocampal area CA1.
5. If necessary, modify the micro-drive body (**Figure 1A**) to accommodate the attachment of the electronic interface board (EIB).
6. Print the micro-drive body, cannula, cone, and lid at high resolution on a 3D printer (ideally with a resolution better than 25 µm), and prepare the printed materials according to the manufacturer's protocols. Use printer resins with high rigidity.

2. Assembling the custom screws and attachments (**Figure 2A, B**)
   1. Using 3D CAD software, load the screw attachment models (**Figure 1E**).
   2. Print the screw attachments at high resolution on a 3D printer (ideally with a resolution of at least 25 µm), and prepare the printed materials according to the manufacturer's protocols. Use printer resins with high rigidity.
   3. Affix the screw attachments to each tetrode-advancing screw (**Figure 1F**) (tetrode-advancing screws are custom manufactured at a machine shop prior to micro-drive construction).
      1. Affix two screw attachments to each screw, with one above and one below the ridge. Ensure that the bottom of each screw attachment contacts the ridge. Hold the screw attachments together with gel cyanoacrylate.
      2. Once affixed, ensure that the screw attachments do not move in the longitudinal axis of the screw but rotate freely with minimal resistance.
3. Assembling the micro-drive body (**Figure 2C, D**)
   1. Using fine, sharp scissors, cut large polyimide tubing (outer diameter: 0.2921 mm, inner diameter: 0.1803 mm) into ~6 cm long sections.
   2. Pass the large polyimide sections through the output holes on the micro-drive cannula so that each tube extends beyond the bottom of the cannula by a few millimeters.
   3. Using a clean 30 G needle, affix the polyimide to the cannula by applying small amounts of liquid cyanoacrylate. Take care not to allow the

cyanoacrylate to enter the inside of the polyimide tube.

NOTE: Dripping liquid cyanoacrylate down into the cannula through the top of the drive body can expedite this process but will require re-clearing of the guide holes later with a fine-tipped drill.

4. Pass the large polyimide tubes from the top of the micro-drive cannula through the appropriate large polyimide holes in the micro-drive body.

5. Slowly push the micro-drive cannula and micro-drive body together until they are adjacent and the cannula/body attachment tabs interlock. Be careful not to kink or damage the polyimide tubes in the process.

NOTE: Each polyimide tube should smoothly pass from the bottom of the cannula out through the top of the micro-drive body. Slight bending is normal, but excessive bending of the polyimide tube can warp the tetrode and prevent it from passing straight into the brain.

6. Affix the micro-drive body and the micro-drive cannula together using cyanoacrylate.

7. Using a new, sharp razor blade, sever the large polyimide tube ends that are extruding from the bottom of the cannula output holes. Ensure that the cut is exactly at the base of the cannula, making the tubes and the cannula bottom flush with one another.

8. Using sharp scissors, cut the large polyimide tubing just above the edge of the inner rim of the drive body at a ~45° angle.

4. Loading the assembled custom screws (**Figure 2E**)

1. Screw each assembled custom screw into the outer holes of the micro-drive body. Ensure the screw guidepost passes through the large hole in the screw attachments. Advance each screw fully until it will not advance further. Pre-lubricating the screws with mineral oil or axle grease is recommended.

2. Using extremely sharp scissors, cut small polyimide tubing (outer diameter: 0.1397 mm, inner diameter: 0.1016) into ~4 cm long sections.

3. Pass the small polyimide sections through the large polyimide tubing already mounted in the micro-drive. Ensure that excess small polyimide tubing protrudes from the top and bottom of each large polyimide tube.

4. Affix the small polyimide tubes to the screw attachments *via* cyanoacrylate, taking care not to let any cyanoacrylate enter into either the large or small polyimide tubes.

5. Using a new, sharp razor blade, sever the small polyimide tube ends that are extruding from the bottom of the cannula holes. Ensure that the cut is exactly at the base of the cannula and that the cut is clean, with nothing blocking the polyimide tube hole.

6. Using sharp scissors, cut the top of the small polyimide a few millimeters above the top of the screw attachment at a ~45° angle. Ensure the cut is clean, with nothing blocking the polyimide tube hole.

5. Loading the tetrodes

1. Prepare the tetrodes (~6 cm in length) using previously described methods[31].

2. Using ceramic- or rubber-tipped forceps, carefully pass a tetrode through one of the small polyimide tubes, leaving ~2 cm protruding from the top of the small polyimide tube.

3. Affix the tetrode to the top of the small polyimide tube *via* liquid cyanoacrylate, taking care not to affix the small and large polyimide tubes together in the process.
4. Retract the screw until it is near the top of the drive.
5. Grab the tetrode wire protruding from the bottom of the drive, and gently kink it at the point where it emerges from the cannula.
6. Advance the screw fully back into the drive.
7. Using very sharp scissors, cut the tetrode wire just above the kink. Under a microscope, ensure that the cut is clean and that the metal of all four tetrodes is exposed.
8. Retract the screw until the tetrode is just secured within the cannula.
9. Repeat steps 1.5.2-1.5.8 for all the screws.
10. Attach the EIB to the EIB support platform *via* small jewelry screws.
11. Connect each electrode of each tetrode to the appropriate port on the EIB.

6. Preparing the micro-drive for surgery
   1. Electrically plate the tetrodes to reduce the electrical impedance using previously described methods[31].
   2. After plating, ensure that each tetrode is housed in the cannula such that the tip of the tetrode is flush with the bottom of each cannula hole.
   3. Slide the micro-drive cone around the completed micro-drive. Attach the micro-drive lid to the micro-drive cone by sliding the cone attachment pole into the lid port.
   4. Orient the cone so that the EIB connectors pass freely through the EIB connection pass-through holes when the lid is closed, and glue the cone in place with cyanoacrylate placed around the base of the cone, taking care not to let any cyanoacrylate enter into any of the cannula output holes. Remove the lid.
   5. Carefully backfill each cannula hole with sterile mineral oil to prevent bodily fluids from entering the polyimide holes after surgical implantation.
   6. Carefully coat the base of the cannula with sterile petroleum jelly. This will serve as a barrier to prevent chemical agents (e.g., dental cement) from entering the exposed brain during the surgery.
   7. Weigh the fully assembled micro-drive, lid, and four bone screws to prepare an equal-weight counterbalance.
   8. Optionally, prior to the surgery, extrude the tetrodes at a distance that is appropriate for reaching the target brain regions once the drive is flush with the skull.

      NOTE: Prior to surgical implantation, sterilize the implant via gas sterilization in ethylene oxide (500-1200 mg/L, 2-4 hrs). All bone screws and surgical instruments should be sterilized via autoclave (121°C, 30 minutes).

2. Surgical implantation

1. Anesthetizing the mouse and mounting it in the stereotaxic apparatus
   1. Place the mouse in a small box with sufficient space to move, and anesthetize the mouse with 3%-4% isoflurane.

NOTE: Other anesthetic agents can be used, but caution should be used due to the age, size, and weight of the juvenile mouse subject.

2. Once the mouse is unresponsive (no response to tail pinch, a ventilation rate of ~60 breaths per minute), remove it from the box, and quickly mount it on the stereotaxic apparatus.

3. Quickly, place the stereotaxic mask over the mouse's snout and maintain anesthesia at 1-3% isoflurane. Apply any veterinary-approved pain relief, such as sustained-release buprenorphine (0.05-0.5 mg/kg subcutaneous), or anti-inflammatory agents, such as carprofen (5-10 mg/kg subcutaneous), prior to initial surgical incision.

4. Fully secure the mouse's head in the stereotaxic apparatus using ear bars. Ensure the skull is level and immobile without placing unnecessary pressure on the mouse's ear canals. Due to the limited ossification of juvenile skull bones, it is possible to cause permanent damage during head fixation.

2. Preparing the mouse for surgery and exposing the skull

1. Protect the mouse's eyes by placing a small volume of synthetic tear gel on each eye and covering each eye with an autoclaved patch of foil.

NOTE: The synthetic tears will keep the eyes moist, while the foil will prevent any light source from causing long-term damage. Thicker synthetic tear solutions are preferred as they can also serve as a barrier to the inadvertent introduction of other potentially toxic surgical solutions (ethanol, dental acrylic, etc.) into the eyes.

2. Using sterile cotton-tipped swabs, apply hair-removal cream over the surgical area to remove the hair from the scalp. Be careful not to get the cream near the eyes. After removing the hair, place a sterile drape over the scalp to secure the surgical area.

3. Using sterile cotton-tipped swabs, clean the scalp *via* three consecutive washes of povidone-iodine (10%) solution followed by isopropyl alcohol (100%).

4. Using a sterile scalpel or fine scissors, remove the scalp.

5. Using sterile cotton-tipped swabs and sterile solutions of saline solution (0.9% NaCl) and hydrogen peroxide, thoroughly clean the skull.

6. Identify bregma, and using the stereotaxic apparatus, carefully mark the target recording locations on the skull with a permanent marker.

3. Opening the cannula hole and attaching the bone anchors

1. Remove the skull overlaying the recording sites. # Due to the thinness of the skull at this age, cut the skull with a scalpel blade; this removes the necessity of using a drill, which may damage the underlying dura. Keep the exposed dura moist with the application of sterile saline solution (0.9% NaCl) or sterile mineral oil. Do not remove or puncture the dura at this stage, as it is sufficiently thin in juvenile mice for the tetrodes to pass through in future steps.

2. Carefully drill pilot holes for four bone screws.

1. Place the bone screws in the extreme lateral and rostral or caudal portions of the skull, where the bone is thickest and the bone screws are sufficiently far away from the micro-drive

implant. For the bone screws, use sterile, fine jewelry screws (e.g., UNM 120 thread, 1.5 mm head).

2. Tightly wind one bone screw with a thin, highly conductive wire that will serve as a ground and be attached to the EIB in step 2.4.6.

3. Using a scalpel blade or carefully using a drill bit, score the skull near the bone screw hole locations. Scoring is important to provide a sufficiently rough surface for the liquid cyanoacrylate to bind in step 2.3.5.

4. Using a sterile screwdriver and sterile screw clamp, thread each sterile bone screw into place, taking care not to pierce the underlying dura**.**

5. Using a sterile 30 G needle, place liquid cyanoacrylate around each bone screw. This effectively thickens the skull where the bone screws have been attached. Take care not to allow any cyanoacrylate to enter into the exposed dura above the recording sites.

4. Lowering and attaching the micro-drive (**Figure 2G**)

1. Mount the completed micro-drive onto the stereotaxic apparatus to be carefully lowered onto the mouse skull. Ensure that the micro-drive cannula will be at the appropriate coordinates when lowered.

2. Lower the micro-drive slowly, moving only in the dorsal/ventral direction. Lower the micro-drive with the tetrodes already advanced out of the cannula holes (step 1.6.6) in order to visualize their entry into the brain; any medial/lateral or rostral/caudal movement when the tetrodes are touching the mouse can bend the tetrodes and cause them to miss their final destination.

3. Once the micro-drive is fully lowered, ensure that the base of the cannula just makes contact with the skull/dura. The layer of petroleum jelly and/or mineral oil will serve as a barrier to cover the exposed dura. If necessary, add sterile petroleum jelly or sterile bone wax to cover excess exposed dura.

4. While holding the micro-drive in place with the stereotaxic apparatus, coat the skull in dental cement to affix the micro-drive base to the implanted bone screws.
NOTE: The dental cement should fully encase all the bone screws and should cover the dental cement anchor ledge on the micro-drive cannula.

5. While the dental cement sets, carefully shape it to prevent sharp corners or edges that may harm the mouse or damage the micro-drive. Ensure there is sufficient dental cement to hold the micro-drive, but eliminate excessive dental cement that will add unnecessary weight.

6. Carefully thread the ground wire through the micro-drive, and attach it to the appropriate slot on the EIB.

7. Once the dental cement is fully set, carefully detach the micro-drive from the stereotaxic apparatus. Place the lid on the micro-drive.

8. With a sterile cotton-tipped swab and sterile saline, clean the mouse.

9. With a sterile cotton-tipped swab, apply a thin layer of antibiotic ointment to any exposed scalp near the implant site.

10. Remove the foil from the mouse's eyes.

11. Remove the mouse from the stereotaxic apparatus, taking care to support the additional weight of the

micro-drive as the mouse is transported to a clean cage.

3. Post-surgery recovery

1. Immediate recovery
    1. Prior to the surgery, prepare the counterbalance system by connecting a 0.75 in diameter PVC pipe, as shown in **Figure 2G**. One arm of the system passes through holes drilled into the lid of the cage, the second arm rests on top of the cage lid, and the third arm extends above and beyond the cage. The topmost arm is capped.
    2. Carefully attach the micro-drive to the counterbalance system (**Figure 2G-I**), and use a counterbalance weight identical to the weight of the micro-drive and bone screws. Run a strong thread or fishing line from a connector attached to the EIB over the three arms of the counterbalance system to the counterbalance weight, which hangs over the topmost arm.
    3. Ensure that the counterbalance is strongly connected to the micro-drive EIB and that there is sufficient line to give the mouse complete access to the entirety of the cage.
    4. Provide nutrient-rich gel in the cage alongside moistened normal rodent chow to ensure rehydration and recovery.
    5. Monitor the mouse until it fully recovers from the surgical anesthesia.
2. Long-term recovery
    1. At all times, when not attached to the recording equipment, ensure that the micro-drive is supported by the counterbalance system. Reduce the counterweight over time, but never remove it entirely to avoid unanticipated stress to the mouse or torque to the bone screws.
    2. To prevent damage to the implant and counterbalance system, house the mouse without the possibility of direct interaction with other mice for the duration of the experiment.
    3. Provide nutrient-rich gel for at least 3 days following surgery, at which point solid food alone will be sufficient.
        1. Due to the overhead requirements of the counterbalance system, do not provide food and water in an overhead wire mesh; place the food on the cage floor, and provide water through the side of the cage. To prevent spoilage, replace the food entirely daily.
    4. Daily, ensure that the mouse has free access to the entirety of the cage and that the counterbalance is robustly and strongly attached to the micro-drive.

Representative Results

The above-described protocol was used to record local field potential signals and single units from multiple brain areas simultaneously in mice, with daily recordings conducted in the same mice from p20 to p60. Reported here are representative electrophysiological recordings from two mice and post-experiment histology demonstrating the final recording locations.

Surgical implantation of the micro-drive into p20 mice

A micro-drive (**Figure 1**) was constructed (**Figure 2**) and surgically implanted into a p20 mouse, as described above. Immediately following the surgery, the mouse was attached to the counterbalance system (**Figure 2G-I**) and allowed

to recover. Once the mouse was fully mobile, the micro-drive was plugged into an *in vivo* electrophysiology recording system. The cables connecting the micro-drive to the recording equipment were suspended above the mouse. Electrophysiological recordings (32 kHz) were obtained across all the channels for 1 h while the mouse behaved naturally in its home cage. Following the recording, the mouse was unplugged from the recording system, reattached to the counterbalance system, and returned to the vivarium with free access to water and chow.

Daily recording of neural activity

Electrophysiological recordings were obtained daily for several weeks to enable the chronic monitoring of the same brain region across the critical developmental windows of p20-p60. Sample raw local field potentials (LFP) from across the chronic recordings are shown in **Figure 3A**,**C**. Isolated single units were simultaneously obtained from multiple tetrodes (**Figure 3B**). Units with similar waveforms were identified across multiple days (**Figure 3B**, middle and right), but due to the potential drift of the recording electrode, it was not possible to definitively claim that the same unit was being identified across days. In a separate mouse implanted at p20 and recorded daily for several weeks, neural activity was examined on a tetrode targeting dorsal area CA1. Large-amplitude ripples and well-isolated single units were identified on each day of the recording (**Figure 4**).These data indicate that stable, high-quality *in vivo* electrophysiological recordings could be from the same mouse across early development.

Histological confirmation of the recording sites and the developmental impact of chronic implantation

Following the final recording day, the mouse was thoroughly anesthetized *via* isoflurane anesthesia followed by a lethal injection of pentobarbital sodium, and a current was passed through the electrode tips to produce small lesions at the recording sites. Post-experiment histological sectioning of the mouse brain allowed the visualization of the final recording sites (**Figure 5A**,**B**). In a separate cohort, three male and three female mice were surgically implanted at p20 as described above. Equal numbers of littermates were left unimplanted and maintained in identical housing conditions. The mice were sacrificed at p62 (6 weeks post-surgery for the implanted cohort). The skulls were carefully cleaned, and external measurements were taken of the bregma-to-lambda distance (**Figure 5C**, top left) and external maximal skull width at lambda (**Figure 5C**, top right). An incision was made along the midline of the skull, and one-half of the skull was removed to excise the brain for mass measurement (**Figure 5C**, bottom right). The height of the skull cavity at bregma was measured from the intact skull half (**Figure 5C**, bottom left). No measure was significantly different between the implanted and unimplanted cohorts (Wilcoxon rank-sum test), indicating that long-term implantation, starting at p20, has no gross impact on the natural development of the skull or brain volume.

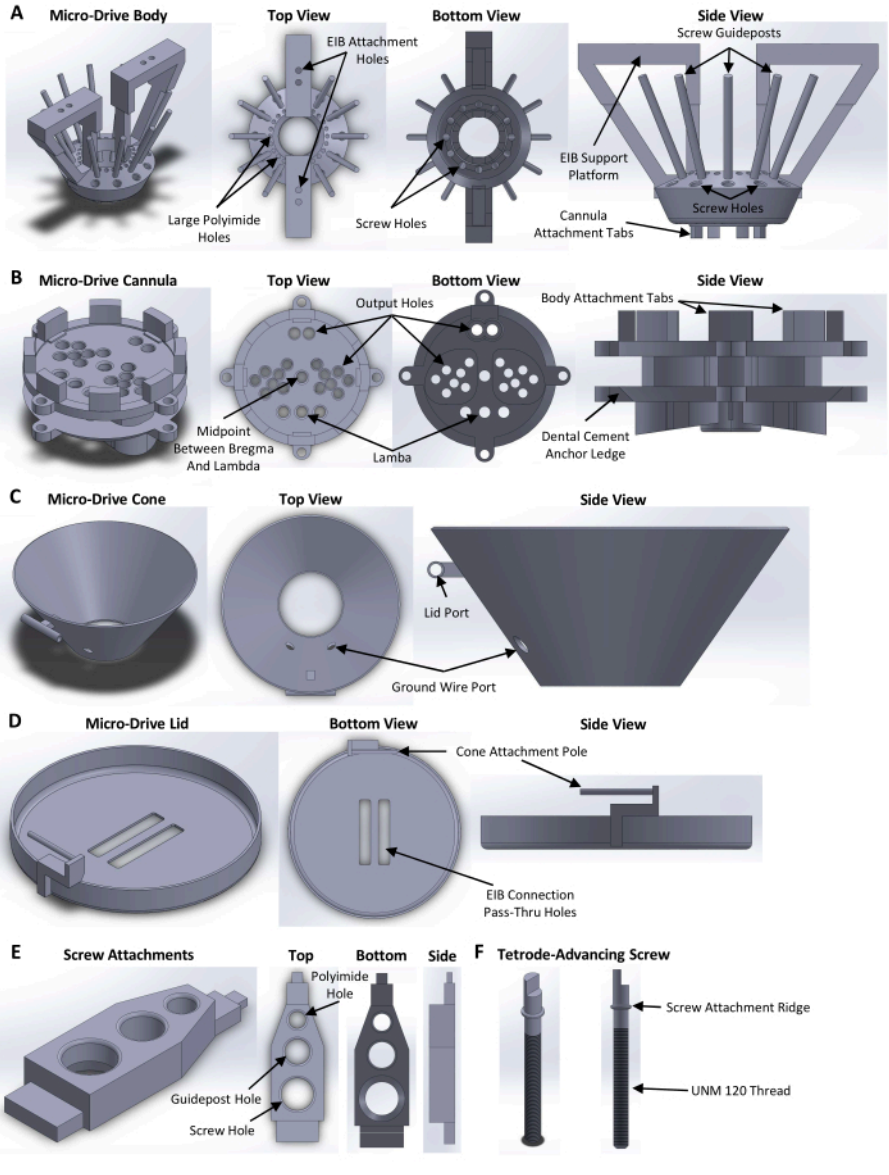

Figure 1: Micro-drive components. Three-dimensional renderings of the (**A**) micro-drive body, (**B**) cannula, (**C**) cone, (**D**) lid, (**E**) screw attachments, and (**F**) tetrode-advancing screw. The critical features of each component are indicated. Measurement details can be extracted from the model files available at https://github.com/Brad-E-Pfeiffer/JuvenileMouseMicroDrive/. Please click here to view a larger version of this figure.

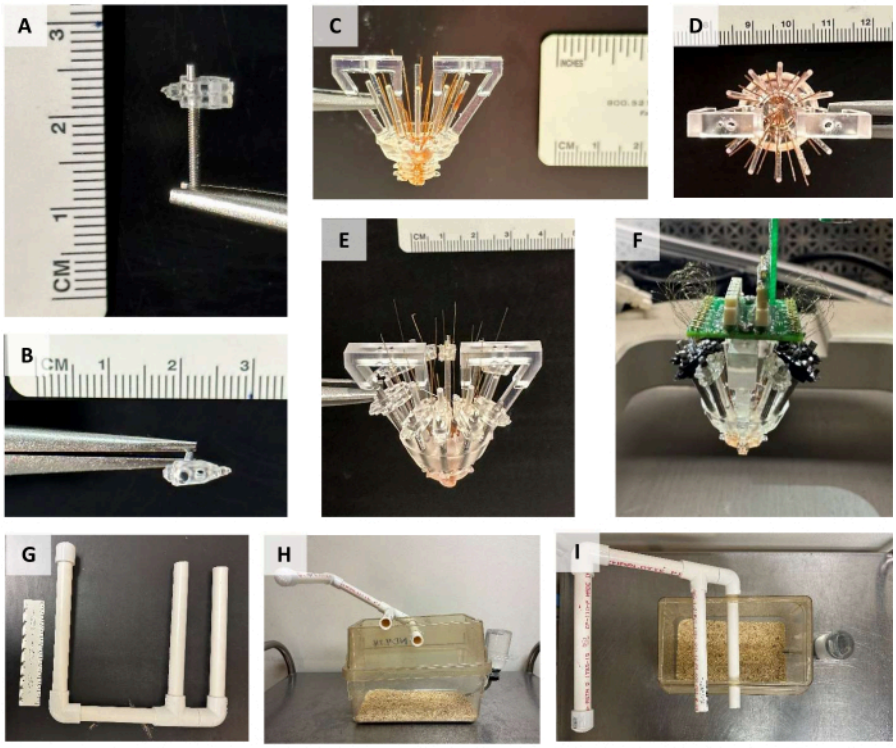

Figure 2: Micro-drive construction. (**A**) Side and (**B**) top view of the tetrode-advancing screw with the top and bottom screw attachments connected. (**C**) Side and (**D**) top view of the micro-drive with the body and cannula attached and the large polyimide tubing running through each cannula hole and trimmed to the bottom of the cannula. (**E**) Side view of the micro-drive with the screws and small polyimide tubing in place. The tops of the small polyimide tubes are trimmed immediately prior to tetrode loading. (**F**) Completed micro-drive attached to the stereotaxic apparatus. The protective cone that would normally surround the micro-drive has been removed for visualization purposes. Note that some of the screw attachments were printed in a black resin for this micro-drive. (**G**) Counterbalance support system. (**H**)Side and (**I**) top view of a mouse cage with the counterbalance support system attached. Please click here to view a larger version of this figure.

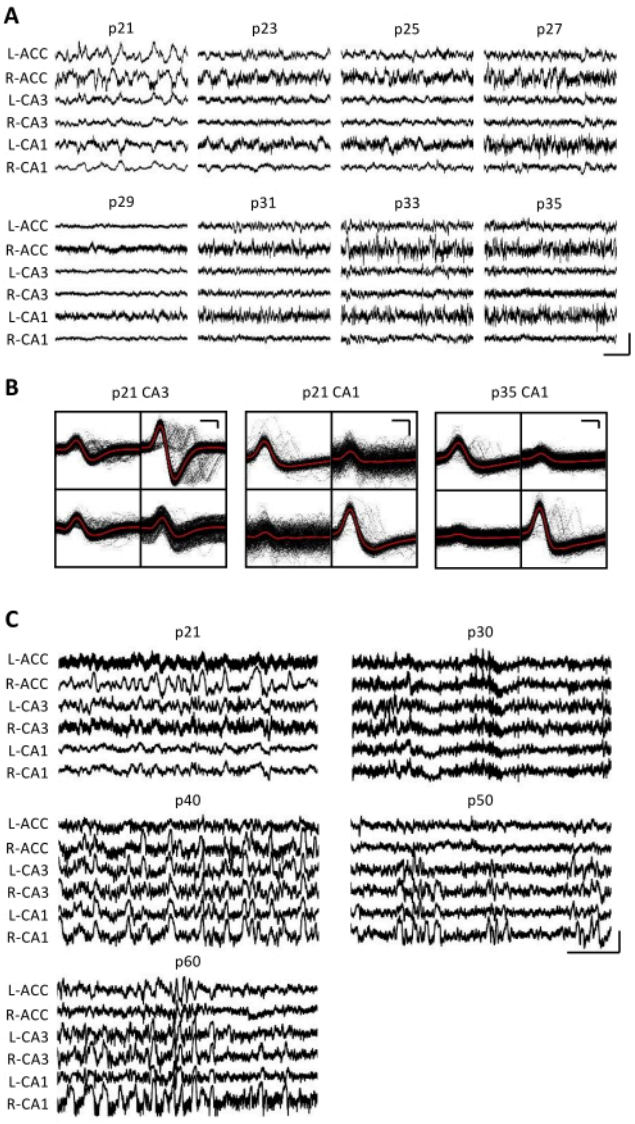

Figure 3: Representative electrophysiological recordings. A p20 mouse was implanted with a micro-drive as described above. Starting on p21 and every day thereafter for 2 weeks, the mouse was attached to the recording apparatus, and neural activity was recorded for at least 1 h. (**A**) Raw local field potential (LFP) recordings from the bilateral (L = left; R = right) anterior cingulate cortex (ACC), hippocampal area CA3 (CA3), and hippocampal area CA1 (CA1). The data were collected every day; for clarity, only data from odd days are displayed. All traces were taken during periods of immobility in the home cage. Scale bar: 1 mV, 2 s. (**B**) Representative single units isolated from hippocampal area CA3 (left) and CA1 (right) for the recordings in panel **A**. All the raw waveforms on each electrode are shown in black; the average is in red. Scale bar: 50 µV, 0.2 ms. (**C**) Representative raw LFP traces for every 10th day until the final recording day at p60 for a second mouse implanted at p20. The data were collected every day; for clarity, only data from every 10th day are displayed. All the traces

were taken during periods of immobility in the home cage. Scale bar: 1 mV, 2 s. Please click here to view a larger version of this figure.

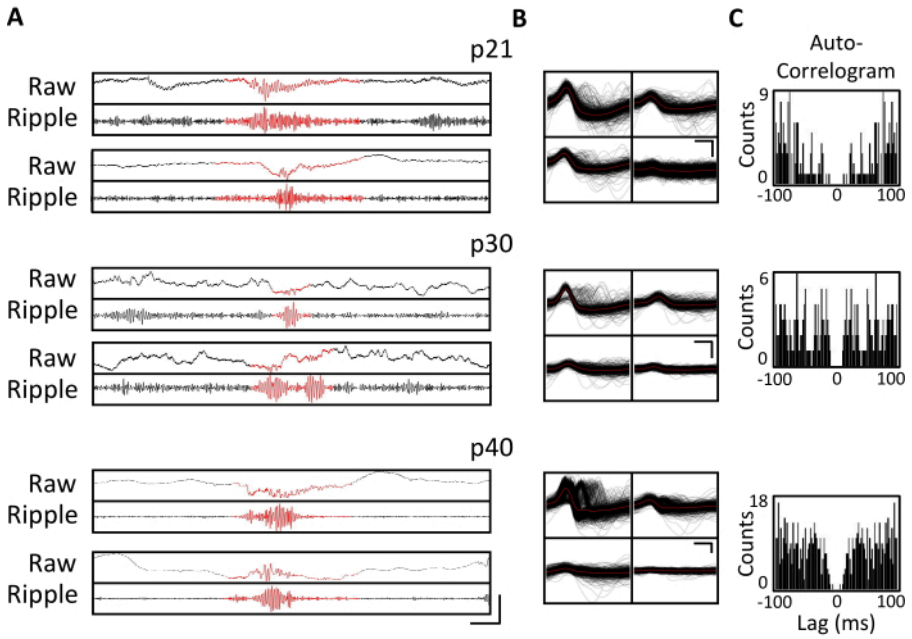

Figure 4. Stability of the chronic recordings. A p20 mouse was implanted with a micro-drive, as described above. Starting on p21 and thereafter for 4 weeks, the mouse was attached to the recording apparatus, and neural activity was recorded for at least 1 h. Shown are data from the tetrodes targeting dorsal hippocampal CA1. (**A**) Raw (top) and ripple-filtered (bottom) LFP for identified ripple events at p21, p30, and p40. To identify ripple events, the raw LFP was band-pass filtered between 125 Hz and 300 Hz, and the ripple events were identified as transient increases in the ripple-band power greater than 3 standard deviations above the mean. The start and end of each ripple were defined as the point when the ripple band power returned to the mean. The identified ripples are shown in red. Scale bar: 100 ms, top-to-bottom: 1,000 µV, 140 µV, 1,800 µV, 180 µV, 9,000 µV, 1,200 µV, 10,000 µV, 1,000 µV. (**B**) A representative single unit from each day from the CA1-targeted tetrode for the recordings in panel **A**. All raw waveforms on each electrode are shown in black; the average is in red. Scale bar 0.2 ms, top-to-bottom: 50 µV, 100 µV, 100 µV. (**C**) Autocorrelogram of all spikes for single units in panel **B**. These data demonstrate stable electrode placement within the hippocampal pyramidal layer across several weeks. Please click here to view a larger version of this figure.

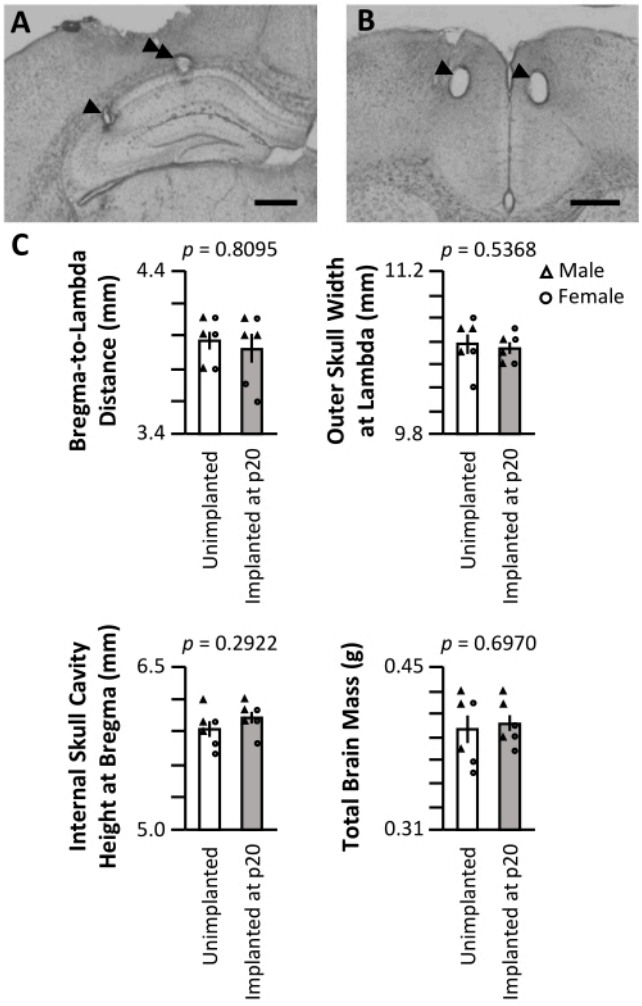

Figure 5: Representative histology and impact on skull development. A p20 mouse was implanted with a micro-drive, as described above. Following the final recording day on p60, electrolytic lesions were produced at the recording sites, and the brain was perfused with 4% paraformaldehyde. To identify the recording sites, 50 µm sections were produced. (**A**) Lesions in CA1 and CA3 of the hippocampus. The arrowhead denotes the CA3 recording site; the double-arrowhead denotes the CA1 recording site. Scale bar: 0.5 mm. (**B**) Lesions in the bilateral ACC. The arrowheads denote the ACC recording sites. Scale bar: 0.5 mm. (**C**) Skull size and brain mass measurements of p62 mice implanted with a micro-drive at p20 (gray) and unimplanted littermates (white). The *p*-value of the Wilcoxon rank-sum test is reported for each measurement. Please click here to view a larger version of this figure.

Discussion

Modern experiments exploring *in vivo* neural circuit function in rodents often utilize extracellular electrophysiology *via* permanently implanted electrodes to monitor the activity of individual neurons (i.e., single units) or local populations (*via* local field potentials, LFP), but such methods are

rarely applied to juvenile mice due to technical challenges. This manuscript describes a method for obtaining *in vivo* electrophysiological recordings in mice across the developmentally critical windows of p20 to p60 and beyond. This methodology involves a manufacturing process for the printing and construction of a micro-drive implant, a surgical implantation procedure, and a post-surgery recovery strategy, all of which are specifically tailored for use in juvenile mice. Several considerations were influential in the development of this protocol, including the small size and relative weakness of juvenile mice compared to their adult counterparts, as well as the reduced ossification of the juvenile mouse skull onto which the micro-drive needed to be attached.

Two primary methods commonly used to perform *in vivo* electrophysiology are arrays of electrodes (e.g., tetrodes) and silicon probes. Silicon probes are lightweight, can provide a large number of recording sites per unit weight, and have been previously utilized in juvenile rats[25]. However, silicon probes are relatively expensive per unit. In contrast, the micro-drive described in this manuscript can be constructed using less than $50 USD in raw materials, making it a cost-effective option for *in vivo* recording. In addition, silicon probes must often be implanted in fixed lines, which prohibits the recording of spatially diverse brain regions. In contrast, the micro-drive design described in this manuscript utilizes independently adjustable tetrodes to accommodate simultaneous recordings in up to 16 different locations with virtually no restriction on the spatial relationship between those locations. This micro-drive design can be easily modified to allow for targeting different locations than those described here by moving the cannula hole extrusions to any desired anterior/posterior and medial/distal location. When targeting alternate brain areas, it is important to note that while the tetrodes will often travel straight, it is possible for these thin wires to deflect slightly as they exit the micro-drive cannula. Thus, the smaller or more ventral a brain region is, the more challenging it will be to successfully target the area with tetrodes.

The micro-drive implant described in this manuscript is foundationally similar to several prior tetrode-based micro-drive designs[23,32,33,34,35] in that the individual tetrodes are affixed to screws, which allow for the fine control of the recording depth of each tetrode. While several features of the current micro-drive design are unique, including the ease of targeting spatially distributed brain areas, the primary novelty of the current manuscript is the description of surgical implantation and post-surgery recovery strategies, which allow for chronic studies of network activity in still-developing juvenile mice. Indeed, the surgery and recovery methodologies described here could be adapted to support other implants in juvenile mice.

To maintain a consistent recording across multiple days, the wires or probes must be rigidly affixed to the skull. While the overall structure of the mouse skull undergoes only minor changes after p20, the skull thickens considerably between ages p20 and p45[36]. Indeed, the skull at p20 is insufficiently rigid to support an attached implant without being damaged. To overcome this biological limitation, this protocol artificially thickens the skull *via* cyanoacrylate during the implantation surgery. Implantation in mice younger than p20 is likely possible using this strategy, but the mouse skull undergoes considerable size and shape changes until roughly p20[36]. Thus, implantation for extended periods in mice younger than p20 is not recommended as the cyanoacrylate and fixed bone screws in the still-developing skull may significantly impact the natural growth of the skull and the underlying brain tissue development. Importantly, in this study, no impact on the

gross measurements of the skull or brain size was observed following chronic implantation starting at p20 (**Figure 5C**).

A critical step in the method described in this manuscript is the post-surgery recovery strategy; according to this strategy, the weight of the implant should be continuously counterbalanced as the mouse matures and undergoes muscular and musculoskeletal system development. Early after implantation, mice are unable to successfully bear the weight of the implant without the counterbalance, leading to malnourishment and dehydration as the mouse cannot adequately reach the food and water sources in its cage. The counterbalance system is easy and inexpensive to construct, trivial to implement, and allows mice of any implantable age to freely explore the entirety of their home cage, thus ensuring adequate nutrition and hydration. As mice age, the amount of counterbalance can be lessened until it can be entirely removed in adult mice; however, the continued use of the counterbalance system is recommended for the duration of the experiment with at least a nominal counterweight attached at all times. While an adult mouse may be able to bear the size and weight of the micro-drive over time, continued natural movement during free behavior with no ameliorating counterweight produces torque and shearing force on the bone screws that anchor the micro-drive onto the skull, making it increasingly likely to become detached, especially during longer chronic experiments.

Two important limitations are of note for the current study. First, to assess the impact of implantation at p20 on skull and brain development, several cohorts of mice were sacrificed after prolonged implantation (**Figure 5C**). While these analyses revealed no significant impact of implantation on the skull cavity size or brain mass (**Figure 5C**), the current study did not examine the skull size or brain mass at multiple time points throughout the early developmental period of p20-p60. While prior work demonstrates that the development of the brain cavity is completed by p20[36], it is possible that implantation at this early window may produce unanticipated changes that are corrected or compensated for by the adult ages that were evaluated here. Second, the experiments that produced the electrophysiological data shown in **Figure 3** and **Figure 4** were not designed to maximize the cell yield. Thus, while the data presented here demonstrate stable, chronic recordings and well-isolated single units, they should not be taken as representative of the maximal potential yield for this device.

Many human neurological and psychiatric disorders manifest during periods of early development or across adolescence, including autism and schizophrenia. However, little is known regarding the circuit-level dysfunction that may underlie these diseases, despite the plethora of mouse models available. The identification of these initial network changes is critical for creating early detection strategies and treatment paradigms. Yet, due to technical challenges, it remains unclear how network function is disrupted across development in mouse models of neuropsychiatric diseases. The micro-drive and recovery strategy described here is designed to support investigations into multi-regional brain network development in the mouse brain and, thus, allow researchers to measure healthy brain development as well as identify alterations to that development in mouse models of disease.

Disclosures

The authors have nothing to disclose.

Acknowledgments

This work was supported by National Institutes of Health R01 NS104829 (B.E.P.), R01 MH117149 (L.J.V.), and

F99NS12053 (L.D.Q.) and the UT Southwestern GSO Endowment Award (R.J.P. and L.D.Q.). The authors thank Jenny Scaria (Texas Tech University Health Sciences Center School of Pharmacy) for technical assistance and Dr. Brendon Watson (University of Michigan) for methodological suggestions.

References

1. Konrad, K., Firk, C., Uhlhaas, P. J. Brain development during adolescence. *Deutsches Arzteblatt International.* **110** (25), 425-431 (2013).
2. Silbereis, J. C., Pochareddy, S., Zhu, Y., Li, M., Sestan, N. The cellular and molecular landscapes of the developing human central nervous system. *Neuron.* **89** (2), 248-268 (2016).
3. Semple, B. D., Blomgren, K., Gimlin, K., Ferriero, D. M., Noble-Haeusslein, L. J. Brain development in rodents and humans: Identifying benchmarks of maturation and vulnerability to injury across species. *Progress in Neurobiology.* **106-107**, 1-16 (2013).
4. Volk, L., Chiu, S.-L., Sharma, K., Huganir, R. L. Glutamate synapses in human cognitive disorders. *Annual Review of Neuroscience.* **38**, 127-149 (2015).
5. Lord, C. et al. Autism spectrum disorder. *Nature Reviews Disease Primers.* **6**, 5 (2020).
6. McCutcheon, R. A., Reis Marques, T., Howes, O. D. Schizophrenia - An overview. *JAMA Psychiatry.* **77** (2), 201-210 (2020).
7. Hopfield, J. J. Neural networks and physical systems with emergent collective computational abilities. *Proceedings of the National Academy of Sciences of the United States of America.* **79** (8), 2554-2558 (1982).
8. Heeger, D. J. Theory of cortical function. *Proceedings of the National Academy of Sciences of the United States of America.* **114** (8), 1773-1782 (2017).
9. Pouget, A., Dayan, P., Zemel, R. Information processing with population codes. *Nature Reviews Neuroscience.* **1**, 125-132 (2000).
10. Averbeck, B. B., Latham, P. E., Pouget, A. Neural correlations, population coding and computation. *Nature Reviews Neuroscience.* **7** (5), 358-366 (2006).
11. Bey, A. L., Jiang, Y.-H. Overview of mouse models of autism spectrum disorders. *Current Protocols in Pharmacology.* **66**, 5.66.1-5.66.26 (2014).
12. Kazdoba, T. M. et al. Translational mouse models of autism: Advancing toward pharmacological therapeutics. *Current Topics in Behavioral Neurosciences.* **28**, 1-52 (2016).
13. Mendoza, M. L., Quigley, L. D., Dunham, T., Volk, L. J. KIBRA regulates activity-induced AMPA receptor expression and synaptic plasticity in an age-dependent manner. *iScience.* **25** (12), 105623 (2022).
14. Bernardet, M., Crusio, W. E. Fmr1 KO mice as a possible model of autistic features. *The Scientific World Journal.* **6**, 1164-1176 (2006).
15. Weaving, L. S., Ellaway, C. J., Gécz, J., Christodoulou, J. Rett syndrome: Clinical review and genetic update. *Journal of Medical Genetics.* **42** (1), 1-7 (2005).
16. Krawczyk, M. et al. Hippocampal hyperexcitability in fetal alcohol spectrum disorder: Pathological sharp waves and excitatory/inhibitory synaptic imbalance. *Experimental Neurology.* **280**, 70-79 (2016).
17. Jaramillo, T. C. et al. Altered striatal synaptic function and abnormal behaviour in Shank3 exon4-9 deletion

mouse model of autism. *Autism Research.* **9** (3), 350-375 (2016).

18. Suh, J., Foster, D. J., Davoudi, H., Wilson, M. A., Tonegawa, S. Impaired hippocampal ripple-associated replay in a mouse model of schizophrenia. *Neuron.* **80** (2), 484-493 (2013).
19. Altimus, C., Harrold, J., Jaaro-Peled, H., Sawa, A., Foster, D. J. Disordered ripples are a common feature of genetically distinct mouse models relevant to schizophrenia. *Molecular Neuropsychiatry.* **1** (1), 52-59 (2015).
20. Marcotte, E. R., Pearson, D. M., Srivastava, L. K. Animal models of schizophrenia: A critical review. *Journal of Psychiatry and Neuroscience.* **26** (5), 395-410 (2001).
21. Makuch, L. et al. Regulation of AMPA receptor function by the human memory-associated gene KIBRA. *Neuron.* **71** (6), 1022-1029 (2011).
22. Dutta, S., Sengupta, P. Men and mice: Relating their ages. *Life Sciences.* **152**, 244-248 (2016).
23. Kloosterman, F. et al. Micro-drive array for chronic in vivo recording: Drive fabrication. *Journal of Visualized Experiments.* (26), 1094 (2009).
24. Buzsáki, G. Large-scale recording of neuronal ensembles. *Nature Neuroscience.* **7** (5), 446-451 (2004).
25. Farooq, U., Dragoi, G. Emergence of preconfigured and plastic time-compressed sequences in early postnatal development. *Science.* **363** (6423), 168-173 (2019).
26. Langston, R. F. et al. Development of the spatial representation system in the rat. *Science.* **328** (5985), 1576-1580 (2010).
27. Wills, T. J., Cacucci, F., Burgess, N., O'Keefe, J. Development of the hippocampal cognitive map in preweanling rats. *Science.* **328** (5985), 1573-1576 (2010).
28. Bjerknes, T. L., Moser, E. I., Moser, M. B. Representation of geometric borders in the developing rat. *Neuron.* **82** (1), 71-78 (2014).
29. Bjerknes, T. L., Dagslott, N. C., Moser, E. I., Moser, M.-B. Path integration in place cells of developing rats. *Proceedings of the National Academy of Sciences.* **115** (7), E1637-E1646 (2018).
30. Jansen, N. A. et al. Impaired θ-γ coupling indicates inhibitory dysfunction and seizure risk in a Dravet syndrome mouse model. *Journal of Neuroscience.* **41** (3), 524-537 (2021).
31. Nguyen, D. P. et al. Micro-drive array for chronic in vivo recording: Tetrode assembly. *Journal of Visualized Experiments.* (26), 1098 (2009).
32. Voigts, J., Siegle, J., Pritchett, D. L., Moore, C. I. The flexDrive: An ultra-light implant for optical control and highly parallel chronic recording of neuronal ensembles in freely moving mice. *Frontiers in Systems Neuroscience.* **7**, 8 (2013).
33. Voigts, J., Newman, J. P., Wilson, M. A., Harnett, M. T. An easy-to-assemble, robust, and lightweight drive implant for chronic tetrode recordings in freely moving animals. *Journal of Neural Engineering.* **17** (2), 026044 (2020).
34. Guardamagna, M. et al. The Hybrid Drive: A chronic implant device combining tetrode arrays with silicon probes for layer-resolved ensemble electrophysiology in freely moving mice. *Journal of Neural Engineering.* **19** (3) (2022).
35. Yamamoto, J., Wilson, M. A. Large-scale chronically implantable precision motorized microdrive array for

freely behaving animals. *Journal of Neurophysiology.* **100** (4), 2430-2440 (2008).

36. Vora, S. R., Camci, E. D., Cox, T. C. Postnatal ontogeny of the cranial base and craniofacial skeleton in male C57BL/6J mice: A reference standard for quantitative analysis. *Frontiers in Physiology.* **6**, 417 (2016).